Modulation by Organic Cosolvent of Microscopic Compositions of Virtual Transition States in the Acylation Stage of Cholesterol Esterase Catalyzed Hydrolysis of Short-Chain *p*-Nitrophenyl Esters

Larry D. Sutton† and Daniel M. Quinn*

Contribution from the Department of Chemistry, University of Iowa, Iowa City, Iowa 52242.
Received December 18, 1989

Abstract: The mechanism for the acylation stage of cholesterol esterase catalyzed hydrolysis of lipid *p*-nitrophenyl esters involves sequential physical (rate constant k_3) and chemical (rate constant k_5) steps that follow substrate binding. For the short-chain esters *p*-nitrophenyl acetate and *p*-nitrophenyl propanoate, the transition states of these steps contribute nearly equally to rate limitation of V/K (acylation) and, hence, the phenomenological transition state is a virtual transition state. For the longer and more specific substrate *p*-nitrophenyl butyrate, the physical step is sufficiently rapid that only the chemical transition state contributes to acylation rate determination. However, upon inhibition of cholesterol esterase catalyzed hydrolysis of *p*-nitrophenyl butyrate by acetonitrile, rate determination of acylation is shifted to a virtual transition state whose composition is similar to those of the *p*-nitrophenyl acetate and *p*-nitrophenyl propanoate reactions. The following changes that accompany inhibition by 10% acetonitrile (v/v) suggest this shift in relative rate determination: (a) $^{D_2O}V/K$ decreases from 2.00 ± 0.02 to 1.55 ± 0.02. (b) The shape of the proton inventory of V/K changes from linear to nonlinear and upward bulging. Least-squares analysis of the proton inventory gives an intrinsic isotope effect $^{D_2O}k_5 = 2.4 \pm 0.3$ and a fractional rate determination by k_5 of 42 ± 2%; the isotope effect is similar to the observed effect (i.e., 2.00) in the absence of acetonitrile. (c) The curvature of the Eyring plot for V/K of PNPB hydrolysis increases markedly when CEase is inhibited by acetonitrile. These results, along with those for *p*-nitrophenyl acetate and *p*-nitrophenyl propanoate, are used herein to construct a model for the reaction dynamics and thermodynamics of the acylation stage of cholesterol esterase catalyzed hydrolysis of short-chain lipid *p*-nitrophenyl esters.

Introduction

In the preceding paper, investigations of the dependence of transition-state structure on reactivity for cholesterol esterase (CEase[1]) catalyzed hydrolysis of a homologous series of lipid *p*-nitrophenyl esters are described.[2] The proton-transfer elements of the deacylation transition state are impervious to change in the fatty acyl chain length of the substrate, since all k_{cat} proton inventories are linear and the intrinsic solvent isotope effects ($^{D_2O}k_{cat}$ values) hover around 2. The acylation transition state, on the other hand, varies greatly with substrate structure. Acylation by short substrates (C_2 and C_3) is rate-limited by a virtual transition state[3-7] that is a composite of contributions from serial isotopically sensitive and isotopically insensitive microscopic transition states. With increasing chain length, parallel pathways that involve aqueous and micelle-bound pools of substrate operate, and for the longest substrates, a single route that involves rate-determining substrate binding from the micelle pool operates.

The virtual transition state that rate limits the acylation stage of CEase-catalyzed hydrolysis of short-chain *p*-nitrophenyl esters can be accounted for by the mechanism in Scheme I. In this mechanism, EA_1 and EA_2 are Michaelis complexes that are interconverted by a reversible, isotopically insensitive isomerization that precedes the chemical catalytic step k_5. When the free energies of the k_3 and k_5 transition states are similar (i.e., within about 2 kcal mol^{-1}), acylation is rate-limited by a virtual transition state that is a weighted average of contributions from the k_3 and k_5 steps. In the preceding paper, the proton inventory technique[8,9] was used to show that the acylation stage of CEase-catalyzed hydrolysis of PNPB is rate-limited by a chemical transition state that is stabilized by simple general-acid–base proton transfer. In this paper, we show that when the hydrolysis of PNPB is inhibited by the organic cosolvent MeCN, acylation is rate-limited by a virtual transition state. The virtual transition state is characterized by measuring solvent isotope effects, temperature effects, and proton inventories, and the results are used to construct a model for acylation reaction dynamics of CEase-catalyzed hydrolysis of short-chain *p*-nitrophenyl esters.

Experimental Section

Materials. Porcine pancreatic CEase (EC 3.1.1.13) was isolated by a modification[2,10] of the procedure developed by Rudd et al.[11] All other materials were described in the preceding paper.[2]

Kinetic Measurements and Data Reduction. Reaction time courses were followed by the methods described in the preceding paper.[2] In addition, kinetics were determined on Hewlett-Packard HP8452A diode-array UV–visible spectrophotometers; reaction temperature was controlled to ±0.05 °C in water-jacketted cell holders with VWR 1140 refrigerated, circulating water baths.

Procedures for calculation of V, K, and V/K and for analysis of proton inventories were described by Sutton et al.[2] Activation thermodynamic parameters ($\Delta H^{\ddagger}$ and $\Delta S^{\ddagger}$) were calculated from nonlinear Eyring plots as described by Acheson et al.[4] Reversible inhibition of CEase by MeCN was characterized with use of the linear transform of the integrated Michaelis–Menten equation described by Stout et al.[12] Inhibition constants were calculated by nonlinear least-squares fitting[13] of V/K versus [I] data to eq 1. The subscripts of $(V/K)_I$ and $(V/K)_0$ denote values

(1) Abbreviations: CEase, cholesterol esterase; AChE, acetylcholinesterase; BuChE, butyrylcholinesterase; PNPA, *p*-nitrophenyl acetate, the C_2 ester; PNPP, *p*-nitrophenyl propanoate, the C_3 ester; PNPB, *p*-nitrophenyl butyrate, the C_4 ester; PNPV, *p*-nitrophenyl valerate, the C_5 ester; PNPC, *p*-nitrophenyl caprylate, the C_6 ester; PNPO, *p*-nitrophenyl octanoate, the C_8 ester; V, maximal velocity, $V_{max} = k_{cat}[E]_T$; K, Michaelis constant; $V/K = k_{cat}[E]_T/K$, pseudo-first-order acylation rate constant when $[S]_0 \leq K/10$; k_E, second-order acylation rate constant, k_{cat}/K; $^{D_2O}V/K$, solvent isotope effect on V/K, $(V/K)^{H_2O}/(V/K)^{D_2O}$; MeCN, acetonitrile; TX100, Triton X-100.

(2) Sutton, L. D.; Stout, J. S.; Quinn, D. M. *J. Am. Chem. Soc.* **1990**, *112*, preceding paper in this issue.

(3) Stein, R. L. *J. Org. Chem.* **1981**, *46*, 3328–3330. This reference and refs 4–7 provide background on the virtual transition-state concept.

(4) Acheson, S. A.; Barlow, P. N.; Lee, G. C.; Swanson, M. L.; Quinn, D. M. *J. Am. Chem. Soc.* **1987**, *109*, 246–252.

(5) Schowen, R. L. In *Transition States of Biochemical Processes*; Gandour, R. D., Schowen, R. L., Eds.; Plenum: New York, 1978; pp 77–114.

(6) Quinn, D. M. *Chem. Rev.* **1987**, *87*, 955–979.

(7) Barlow, P. N.; Acheson, S. A.; Swanson, M. L.; Quinn, D. M. *J. Am. Chem. Soc.* **1987**, *109*, 253–257.

(8) Schowen, K. B. J. In *Transition States of Biochemical Processes*; Gandour, R. D., Schowen, R. L., Eds.; Plenum: New York, 1978; pp 225–283.

(9) Schowen, K. B.; Schowen, R. L. *Methods Enzymol.* **1982**, *87*, 551–606.

(10) Sutton, L. D.; Stout, J. S.; Hosie, L.; Spencer, P. S.; Quinn, D. M. *Biochem. Biophys. Res. Commun.* **1986**, *134*, 386–392.

(11) Rudd, E. A.; Mizuno, N. K.; Brockman, H. L. *Biochim. Biophys. Acta* **1987**, *918*, 106–114.

* To whom correspondence should be addressed.
† Present address: Department of Pathology, University of Iowa Hospitals and Clinics, Iowa City, IA 52242.

0002-7863/90/1512-8404$02.50/0

Scheme I. Kinetic Mechanism for Acylation of CEase by Short *p*-Nitrophenyl Esters

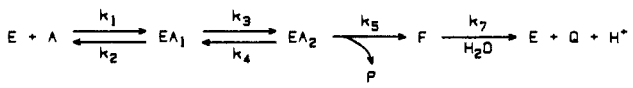

Table I. MeCN Inhibition Constants for CEase-Catalyzed Hydrolysis of Lipid *p*-Nitrophenyl Esters

substrate	K_i[a]	substrate	K_i[a]
PNPA	0.53 ± 0.07	PNPV	2.4 ± 0.5
PNPP	0.67 ± 0.04	PNPC	3.6 ± 0.5
PNPB	4.0 ± 0.4	PNPO	4.8 ± 0.4
PNPB[b]	3.1 ± 0.5		

[a] Inhibition constants are given in percent v/v. Reaction conditions are as described in the legend of Figure 1. [b] Inhibition constant measured in buffered D_2O at pD 7.56.

Table II. Effect of MeCN on Solvent Isotope Effects and Proton Inventories for V/K of CEase-Catalyzed Hydrolyses of Short-Chain *p*-Nitrophenyl Esters

substrate	% MeCN (v/v)	$^{D_2O}k_E$[a]	$^{D_2O}k_5$[b]	C
PNPV	0	1.41 ± 0.03	1.41 ± 0.03	nd[c]
	10	1.39 ± 0.02	1.39 ± 0.02	nd[c]
PNPB	0	2.00 ± 0.02	2.00 ± 0.02	−0.1 ± 0.2
	10	1.55 ± 0.02	2.4 ± 0.3	1.4 ± 0.1
PNPP	0	2.1 ± 0.1	2.8 ± 0.1	0.7 ± 0.1
	4	1.89 ± 0.02	2.6 ± 0.3	0.7 ± 0.3
PNPA	0	1.81 ± 0.03	2.12 ± 0.05	0.5 ± 0.2
	4	2.07 ± 0.03	2.6 ± 0.5	0.5 ± 0.3

[a] Observed solvent isotope effect on k_{cat}/K. [b] Intrinsic solvent isotope effect. Proton inventories for PNPV and for PNPB in the absence of MeCN are linear and were fit to eq 5 of the text. All other proton inventories were fit to eq 7 of the text. Intrinsic solvent isotope effects were calculated from these fits. [c] Not determined.

$$(V/K)_I = (V/K)_0 \frac{K_I + \beta[I]}{K_I + [I]} \quad (1)$$

measured in the presence of MeCN of various concentrations [I] and in the absence of MeCN, respectively, and β is the residual V/K at saturating MeCN.

Results

Acetonitrile Inhibition. MeCN behaves predominantly as a competitive inhibitor of CEase-catalyzed hydrolysis of lipid *p*-nitrophenyl esters, as shown by the Lineweaver–Burk pattern for PNPB that is displayed in Figure 1. Lineweaver–Burk patterns for PNPV, PNPC, and PNPO are also consistent with competitive inhibition. K values exceed substrate solubilities for PNPA and PNPP,[2] so that the patterns for these substrates cannot be determined. Since MeCN inhibition is competitive for the other esters, it is assumed also so for PNPA and PNPP. Inhibition constants were determined by fitting V/K versus [I] data to eq 1 and are given in Table I. However, inhibition is not due just to competition between MeCN and substrate for binding to the free enzyme, since Figure 2 shows that as CEase is increasingly inhibited by MeCN, the observed solvent isotope effect ($^{D_2O}V/K$) decreases. The suppression of $^{D_2O}V/K$ by MeCN is not due to a solvent isotope effect on K_i for MeCN inhibition, since K_i is smaller in D_2O than in H_2O (cf. Table I), and hence, the suppression of the isotope effect is even greater than that shown in Figure 2.

Proton Inventories. Proton inventories of V/K for CEase-catalyzed hydrolysis of PNPB in the absence and presence of 10% MeCN (v/v) are shown in Figure 3. The proton inventory in the absence of MeCN is linear and the solvent isotope effect $^{D_2O}V/K = 2.00$, but in the presence of MeCN $^{D_2O}V/K$ is 1.55 and the proton inventory bulges upward. Results of proton inventories

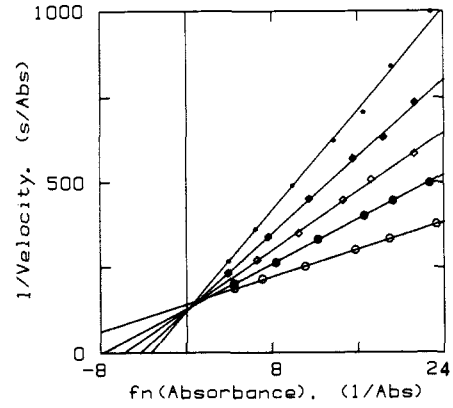

Figure 1. Competitive inhibition of CEase-catalyzed hydrolysis of PNPB by MeCN. MeCN concentrations (v/v): open circles, no MeCN; closed circles, 1.6% MeCN; open diamonds, 3.2% MeCN; closed diamonds, 4.8% MeCN; asterisks, 6.4% MeCN. Reactions were run on a Zymatel robotics system[2,14] at 25.08 ± 0.02 °C in 2.50 mL of 0.1 M sodium phosphate buffer, pH 7.02, that contained 0.1 N NaCl, 1 mM TX100, $[PNPB]_0$ = 300 μM, and 13 μg mL^{-1} CEase.

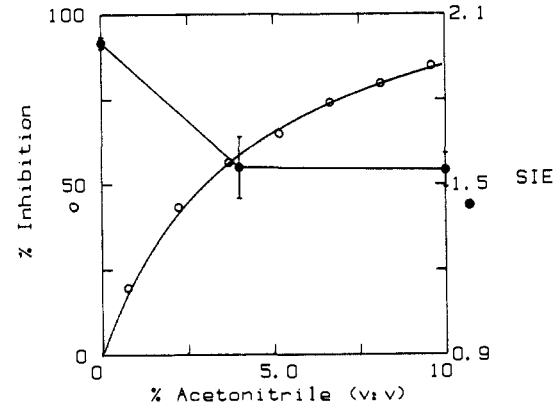

Figure 2. Decrease in solvent deuterium isotope effect on V/K (closed circles) as the extent of inhibition by MeCN (open circles) increases for CEase-catalyzed hydrolysis of PNPB. Except for reactions that contained 10% MeCN (v/v), V/K values were calculated by fitting time courses to the integrated Michaelis–Menten equation.[2,12] For reactions that contained 10% MeCN (v/v), time courses were fit to a first-order equation.[2] SIE denotes the solvent isotope effect on V/K, $^{D_2O}V/K$. Reaction conditions are given in the legend of Figures 1 and 3.

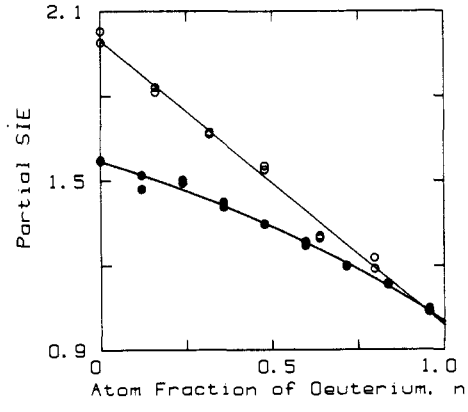

Figure 3. Proton inventories for CEase-catalyzed hydrolysis of PNPB in the absence (open circles) and presence (closed circles) of 10% MeCN (v/v). Time courses were fit to the integrated Michaelis–Menten equation[2,12] and to a first-order function[2] in the absence and presence of MeCN, respectively. The partial solvent isotope effect (SIE) is $^{n}k_E = k_{E,n}/k_{E,l}$. Reactions were run on a Zymatel robotics system[2,14] in 0.1 M sodium phosphate buffer that contained 0.1 N NaCl and 1 mM TX100 at pH 7.00 in H_2O, pD 7.56 in D_2O, and equivalent pL[15] (L = H, D) in H_2O–D_2O mixtures. Reactions without MeCN contained $[PNPB]_0$ = 0.4 mM and 26 μg mL^{-1} CEase and were run at 24.88 ± 0.02 °C; reactions in the presence of MeCN contained 13 μg mL^{-1} CEase and $[PNPB]_0$ = 0.3 mM and were run at 24.98 ± 0.02 °C.

(12) Stout, J. S.; Sutton, L. D.; Quinn, D. M. *Biochim. Biophys. Acta* **1985**, *837*, 6–12.
(13) Wentworth, W. E. *J. Chem. Educ.* **1965**, *42*, 96–103.

Table III. Activation Thermodynamics for CEase-Catalyzed Hydrolysis of PNPB

kinetic parameter	% MeCN (v/v)	activation parameters[a]			
		ΔH_1^*	ΔS_1^*	ΔH_2^*	ΔS_2^*
V/K	0	0.8 ± 0.9	−59 ± 2	25 ± 1	20 ± 1
V/K	10	0.0 ± 0.1	−66 ± 1	28 ± 1	35 ± 2
V	0	1.1 ± 0.9	−80 ± 3	10 ± 2	−49 ± 4

[a] Units: activation enthalpies, kcal mol^{-1}; activation entropies, cal K^{-1} mol^{-1}. Subscripts 1 and 2 of activation parameters for V/K correspond to 3E and 5E, respectively, of eq 10 of the text. See the Experimental Section and the legend of Figure 4 for reaction conditions.

for CEase-catalyzed hydrolyses of four lipid *p*-nitrophenyl esters are given in Table II. These results will be dealt with in detail in the Discussion.

Temperature Dependence of Acylation. Figure 4A shows the Eyring plot[16] for V of CEase-catalyzed hydrolysis of PNPB, and Figure 4B shows Eyring plots for V/K in the presence and absence of 10% MeCN (v/v). In the absence of MeCN, the Eyring plots for V and V/K are slightly concave downward. In the presence of 10% MeCN (v/v), the curvature of the Eyring plot for V/K increases dramatically. The three Eyring plots were fit to a nonlinear Eyring equation that is based on a virtual transition-state model, as described in the Discussion, and the resulting activation thermodynamics parameters are gathered in Table III.

Discussion

The investigations described in this paper further illuminate the reaction dynamics of the acylation stage of CEase-catalyzed hydrolysis of short-chain lipid *p*-nitrophenyl esters. V/K for the mechanism of Scheme I is given by eq 2. In the right-most

$$V/K = \frac{k_1k_3k_5[E_T]}{k_2(k_4 + k_5) + k_3k_5} = \frac{k_1k_3k_5[E_T]}{k_2(k_4 + k_5)} \qquad (2)$$

expression for V/K, $k_3 << k_2$ is assumed; i.e., binding does not contribute to rate determination. This assumption is supported by the following considerations: (1) The solvent isotope effect $^{D_2O}V/K = 2$ for PNPB hydrolysis arises from a single transition-state proton transfer, as indicated by the linear proton inventory of Figure 3. If an isotopically insensitive step such as binding were also contributing prominently to rate determination, then the proton inventory would be nonlinear and upward bulging. (2) As described in the preceding paper,[2] $k_{cat}/K = 1.25 \times 10^6$ M^{-1} s^{-1} for PNPC, the C_6 ester, and $^{D_2O}V/K = 1.41$. The moderate solvent isotope effect indicates that a chemical transition state is at least partially rate-determining. Hence, the bimolecular rate constant for binding must be larger than k_{cat}/K. As the ester is sequentially shortened by a methylene unit, k_{cat}/K decreases and the $^{D_2O}k_{cat}/K$ rises to ~2, which indicates that chemistry increasingly determines the rate. Therefore, binding does not contribute to acylation rate determination for PNPA, PNPP, and PNPB.

As Figure 2 shows, the solvent isotope effect on V/K for PNPB hydrolysis decreases with increasing inhibition by MeCN. This observation and the nonlinear proton inventory of Figure 3 in the presence of MeCN suggest that successive physical and chemical transition states contribute to rate determination; i.e., acylation is rate-determined by a virtual transition state.[3-7] Equation 2 can be used to provide a quantitative accounting of the PNPB proton inventories of Figure 3. Consider the reciprocal of eq 2:

$$k_E^{-1} = \frac{k_2}{k_1k_3} + \frac{k_2k_4}{k_1k_3k_5} = k_{3E}^{-1} + k_{5E}^{-1} \qquad (3)$$

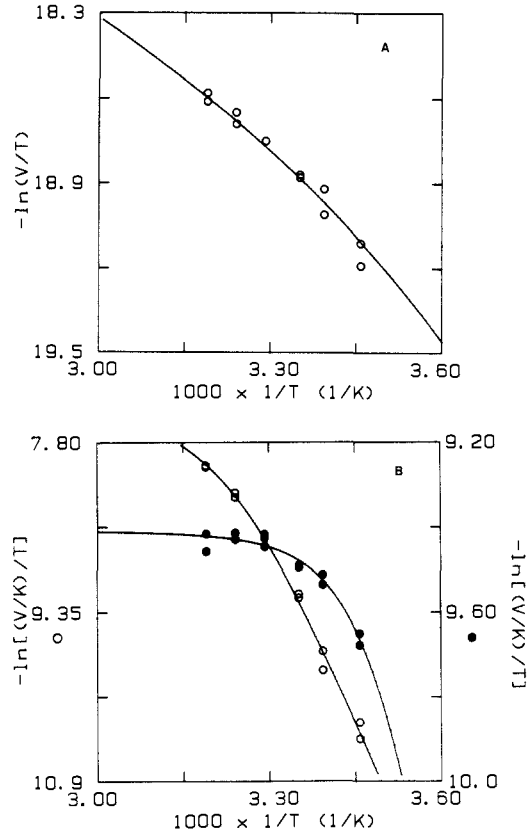

Figure 4. Eyring plots for V (A) and V/K (B) of CEase-catalyzed hydrolysis of PNPB. Open circles and closed circles are for reactions in the absence and presence of 10% MeCN (v/v), respectively. Time courses were fit to the integrated Michaelis–Menten equation[2,12] and to a first-order function[2] in the absence and presence of MeCN, respectively. Reactions were run at pH 7.02 and at the indicated temperatures (as reciprocals) in 1.00 mL of 0.1 M sodium phosphate buffer that contained 0.1 N NaCl and 1 mM TX100. CEase concentrations were 0.64 and 3.2 μg mL^{-1}, respectively, and $[PNPB]_0$ values were 400 and 50 μM, respectively, in the absence and presence of MeCN.

Equation 3 emphasizes that k_E ($=k_{cat}/K = (V/K)/[E_T]$) contains contributions for conversion of the free E + free A reactant state to the successive physical (i.e., $k_{3E} = k_1k_3/k_2$) and chemical (i.e., $k_{5E} = k_1k_3k_5/k_2k_4$) transition states.

For PNPB, the k_5 transition state is prominently rate-determining in the absence of MeCN and is stabilized by a single proton bridge, as the linear proton inventory of Figure 3 shows. Acylation reaction dynamics are, therefore, dominated by k_{5E}, and the requisite form of the Gross–Butler equation[8,9] is given by the following expression, in which $K_{1,3} = k_1k_3/k_2k_4$, n is the atom fraction of deuterium in mixed H_2O–D_2O buffers, and $k_{5,0}$ is k_5 in H_2O (i.e., $n = 0$):

$$k_{E,n} = K_{1,3}k_{5,0}(1 - n + n\phi^T_5) \qquad (4)$$

On division of both sides of eq 4 by $k_{E,1}$, the rate constant in D_2O, one gets the dependence of the partial solvent isotope effect ($^nk_E = k_{E,n}/k_{E,1}$) on n:

$$^nk_E = {}^{D_2O}k_5(1 - n + n\phi^T_5) \qquad (5)$$

The proton inventory was fit by linear least-squares analysis[17] to eq 5, from which the intrinsic solvent isotope effect $^{D_2O}k_5 = 2.00$ was calculated (cf. Table II).

The proton inventory for k_E of CEase-catalyzed hydrolysis of PNPB in the presence of 10% MeCN (v/v) is nonlinear and upward bulging (cf. Figure 3), and the observed solvent isotope effect falls to $^{D_2O}k_E = 1.55$. Equation 3 can readily accommodate these observations if both k_{3E} and k_{5E} are kinetically significant, and again the k_5 transition state is stabilized by a single proton

(14) Quinn, D. M.; Sutton, L. D.; Kinzelman, T. J. *Am. Biotechnol. Lab.* **1988**, *6*, 33–37.

(15) Buffers in D_2O and H_2O are equivalent when the concentrations of all solutes in the isotopic buffers are the same, in which case the pD of the D_2O buffer is said to be equivalent to the pH of the H_2O buffer.[8,9] In this study, the pD of the D_2O buffer is greater than that of the H_2O buffer by 0.5 pH unit.

(16) Glasstone, S.; Laidler, K. J.; Eyring, H. *The Theory of Rate Processes*; McGraw-Hill: New York, 1941.

(17) Young, H. D. *Statistical Treatment of Experimental Data*; McGraw-Hill: New York, 1962; pp 115–126.

transfer, as described in eq 6. From eq 6 one can derive an

$$k_{E,n}^{-1} = k_{3E}^{-1} + [k_{5E}(1 - n + n\phi^{T}_{5})]^{-1} \quad (6)$$

expression for $k_{E,1}$. Multiplication of both sides of eq 6 by $k_{E,1}$, followed by extensive algebraic manipulation, produces the following equation for the dependence of the partial solvent isotope effect on n:

$$^{n}k_{E} = \frac{(f_3 + f_5{}^{D_2O}k_5)(1 - n + n\phi^{T}_{5})}{f_5 + f_3(1 - n + n\phi^{T}_{5})} = \frac{(^{D_2O}k_5 + C)(1 - n + n\phi^{T}_{5})}{1 + C(1 - n + n\phi^{T}_{5})} \quad (7)$$

The right-hand side of eq 7 is cast in two equivalent forms. In the first, f_3 and f_5 are the respective fractions of rate determination by the serial k_3 and k_5 transition states;[18] in the second, $C = k_5/k_4$ is the commitment of EA_2 to proton-transfer catalysis (cf. Scheme I).[18] Since $^{D_2O}k_5 = 1/\phi^{T}_{5}$ and $f_3 + f_5 = 1$, eq 7 contains just two adjustable parameters. The proton inventory for CEase-catalyzed hydrolysis of PNPB in the presence of 10% MeCN (v/v) was fit by nonlinear least-squares procedures[13] to eq 7. The fit is displayed in Figure 3, and the calculated parameters are gathered in Table II. The intrinsic isotope effect is $^{D_2O}k_5 = 2.4 \pm 0.3$, which is similar to that in the absence of MeCN. The commitment $C = 1.4 \pm 0.1$ is consistent with $42 \pm 2\%$ rate determination by the chemical transition state of the k_5 step. The proton inventory for PNPB hydrolysis in the absence of MeCN was also fit to eq 7, and the results are given in Table II. The commitment $C = -0.1 \pm 0.2$ is within error of zero, an unsuprising observation when one notes that when $C = 0$ eq 7 reduces to the linear eq 5. For PNPA and PNPP, the proton inventories are nonlinear in both the presence and absence of MeCN, as the data in Table II indicate, and the commitments are consistent with $67 \pm 13\%$ and $59 \pm 10\%$ rate determination by the k_5 transition state of the respective reactions.

The effect of addition of MeCN is to shift acylation rate determination of PNPB hydrolysis from the transition state of the k_5 step to a virtual transition state that is a weighted average of the k_3 (58%) and k_5 (42%) microscopic transition states. The decrease of the solvent isotope effect as inhibition by MeCN increases (cf. Figure 2) can be accommodated by this model. Assume that the commitment is a function of fractional inhibition:

$$C = \frac{C_{lim}[I]}{K_I + [I]} \quad (8)$$

The commitment $C = 1.4 \pm 0.1$ calculated from the proton inventory of Figure 3 was determined at a fractional inhibition of 0.71 ± 0.02 (calculated from the K_I of Table I), and therefore, $C_{lim} = 1.96 \pm 0.15$. This value of C_{lim} is used in the following equation, which comes from eq 7 when $n = 1$, to describe the dependence of $^{D_2O}k_E$ on [I]:

$$^{D_2O}k_E = \frac{^{D_2O}k_5 + C}{1 + C} = \frac{^{D_2O}k_5 + \frac{C_{lim}[I]}{K_I + [I]}}{1 + \frac{C_{lim}[I]}{K_I + [I]}} \quad (9)$$

In the absence of MeCN, $^{D_2O}k_E = {}^{D_2O}k_5 = 2.00 \pm 0.02$ (cf. Figure 2 and Table II). When [MeCN] = 4% and 10% (v/v), the calculated solvent isotope effects are 1.51 ± 0.09 and 1.42 ± 0.08, respectively, which match within experimental error the observed values of 1.56 ± 0.11 and 1.55 ± 0.06.

Equation 3 also provides a means for describing the temperature dependence of the kinetics of CEase-catalyzed hydrolysis of PNPB. By using the Eyring equation[16] [$k = (k_B T/h)e^{-\Delta G^{\ddagger}/RT}$], one can derive the following expression for the dependence of k_E on T:

$$-\ln \frac{k_E}{T} = \ln (Ae^{\Delta H_{3E}^{\ddagger}/RT} + Be^{\Delta H_{5E}^{\ddagger}/RT}) \quad (10)$$

(18) The fractions of rate determination by the k_3 and k_5 transition states are given by the following expressions: $f_5 = k_{3E}/(k_{3E} + k_{5E})$ and $f_3 = 1 - f_5 = k_{5E}/(k_{3E} + k_{5E})$. Since $C = k_5/k_4$, $f_3 = C/(1 + C)$ and $f_5 = 1/(1 + C)$.

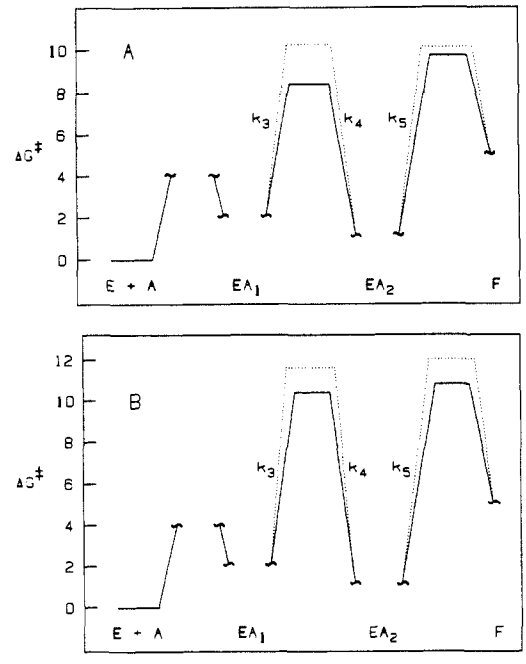

Figure 5. Free energy profiles for the acylation stage of CEase-catalyzed hydrolysis of short-chain *p*-nitrophenyl esters. Standard states of 1 M for all species were used to calculate free energies of activation. Tildes denote that the free energy of the indicated state is unknown. The designation of states along the bottom of the diagrams corresponds to that in the Scheme I mechanism. A. The solid and dotted lines are the profiles for the PNPB reactions in the absence and presence of 10% MeCN (v/v), respectively. In the absence of MeCN, the free energy difference of the transition states of the k_5 and k_3 steps is 1.3 kcal mol^{-1}, which is a lower limit that is consistent with the observation that the chemical transition state is solely rate-determining. B. The solid and dotted lines are the profiles for the PNPA reaction in the absence and presence of 4% MeCN, respectively.

In this equation, $A = (h/k_B)e^{-\Delta S_{3E}^{\ddagger}/R}$ and $B = (h/k_B)e^{-\Delta S_{5E}^{\ddagger}/R}$ and the subscripts of the entropies and enthalpies denote that the parameters describe the activation thermodynamics of conversion of the free E + free A reactant state to the successive transition states of the k_3 and k_5 steps. Parts A and B of Figure 4 show fits to eq 10 for V and V/K of CEase-catalyzed hydrolysis of PNPB.[4] These fits are curvilinear and yield the activation parameters tabulated in Table III. The curvature of the Eyring plot for V/K increases markedly when MeCN inhibits the enzyme, as shown in Figure 4B. Hence, the Eyring plots, like the proton inventories of Figure 3 and the changes in $^{D_2O}V/K$ of Figure 2, signal that a dramatic change in acylation reaction dynamics accompanies MeCN inhibition of CEase-catalyzed hydrolysis of PNPB.

Figure 5 shows free energy diagrams for the acylation stage of CEase-catalyzed hydrolysis of the short-chain esters PNPA and PNPB. The diagrams provide succinct visual presentations of the dynamics of the two reactions and of the way that reaction dynamics respond to MeCN inhibition. The following discussion provides the background for construction of the free energy diagrams of Figure 5. The relative free energies of the transition states of the k_3 and k_5 steps are calculated with use of the following equation, which is derived from the Eyring equation:[6,16,19]

$$\Delta\Delta G^{\ddagger} = \Delta G_{5E}^{\ddagger} - \Delta G_{3E}^{\ddagger} = -RT \ln C \quad (11)$$

The relationship of the phenomenological free energy of activation,

(19) The free energies of activation in eq 11 are with respect to the free E + free A reactant state. The following logic is used to derive the equation:

$$C = k_5/k_4 = \frac{k_1k_3k_5}{k_2k_4} \Big/ \frac{k_1k_3}{k_2} = k_{5E}/k_{3E} \quad (i)$$

$$k_{5E}/k_{3E} = e^{-\Delta\Delta G^{\ddagger}/RT} = e^{-(\Delta G_{5E}^{\ddagger} - \Delta G_{3E}^{\ddagger})/RT} \quad (ii)$$

Equation 11 is the natural logarithm transform of eq ii.

$\Delta G_E^{\ddagger}$, to the microscopic activation free energies of eq 11 is derived from eq 3, again with use of the Eyring equation:[6,16]

$$e^{\Delta G_E^{\ddagger}/RT} = e^{\Delta G_{3E}^{\ddagger}/RT} + e^{\Delta G_{5E}^{\ddagger}/RT} \quad (12)$$

Equations 11 and 12 can be solved for the microscopic free energies of activation in terms of measurable quantities:

$$\Delta G_{3E}^{\ddagger} = \Delta G_E^{\ddagger} + RT \ln f_3 \quad (13)$$

$$\Delta G_{5E}^{\ddagger} = \Delta G_E^{\ddagger} + RT \ln f_5 \quad (14)$$

The activation free energy $\Delta G_E^{\ddagger}$ is calculted from observed values of k_E,[2] and values of f_3 and f_5 are available from fits of proton inventories to eq 7. Equations 13 and 14 were used to calculate the free energies of the k_3 and k_5 transition states, respectively, with respect to the free E + free A reactant state.

In the absence of MeCN, the PNPA reaction traverses successive transition states of nearly equal free energy, with the chemical transition state dominating rate determination by 400 ± 200 cal mol^{-1}. For the PNPP reaction (energy diagram not shown), the k_5 transition state dominates by 210 ± 80 cal mol^{-1}. For the PNPB, which has a 7.5-fold higher V/K than does PNPA,[2] the chemical transition state is rate-determining. Therefore, as CEase specificity increases on extension of the acyl chain from C_2 (PNPA) to C_4 (PNPB), both the k_3 and k_5 transition states are stabilized, but with k_3 the primary beneficiary. Since k_3 is isotopically insensitive, it is reasonable to assign a substrate-triggered enzyme isomerization (induced fit[20]) to the k_3 step.

MeCN inhibition has different effects on the acylation dynamics of PNPA and PNPP reactions, on the one hand, and the PNPB reaction, on the other. As the free energy diagrams show, MeCN inhibition brings the k_3 and k_5 transition states of the PNPB reaction into balance by decreasing k_3 more than k_5, so that both contribute to rate determination. When the free energies of the k_3 and k_5 transition states are already balanced, as in the free energy diagrams of the PNPA reaction, MeCN has no effect on their relative energies.

Conclusion. As discussed in the preceding paper, there are regions of sequence similarity among CEase,[21] BuChE,[22] and AChE.[23] This structural similarity apparently has important functional consequences. Rosenberry suggested that at least for neutral ester substrates induced fit is a prominent component of the acylation reaction dynamics of AChE catalysis.[24,25] This suggestion is supported by pH-rate and solvent isotope effect investigations of AChE-catalyzed hydrolysis of anilides and esters.[4,6,7,26,27] The work described in this paper indicates that CEase utilizes a similar strategy for the generation of catalytic power. Evidently, induced fit not only poises the CEase active site for subsequent stabilization of chemical transition states but also provides the means by which the enzyme expresses substrate specificity.

Acknowledgment. This research was supported by NIH Grant HL30089 and by a Research Career Development Award to D.M.Q. from the National Heart, Lung and Blood Institute of NIH (HL01583, 1985-1990).

(20) Koshland, D. E., Jr. *Proc. Natl. Acad. Sci. U.S.A.* **1958**, *44*, 98-104.

(21) Kissel, J. A.; Fontaine, R. N.; Turck, C. W.; Brockman, H. L.; Hui, D. Y. *Biochim. Biophys. Acta* **1989**, *1006*, 227-236.

(22) Lockridge, O.; Bartels, C. F.; Vaughan, T. A.; Wong, C. K.; Norton, S. E.; Johnson, L. L. *J. Biol. Chem.* **1987**, *262*, 549-557.

(23) Schumacher, M.; Camp, S.; Maulet, Y.; Newton, M.; MacPhee-Quigley, K.; Taylor, S. S.; Friedmann, T.; Taylor, P. *Nature* **1986**, *319*, 407-409.

(24) Rosenberry, T. L. *Adv. Enzymol. Relat. Areas Mol. Biol.* **1975**, *43*, 103-218.

(25) Rosenberry, T. L. *Proc. Natl. Acad. Sci. U.S.A.* **1975**, *72*, 3834-3838.

(26) Quinn, D. M.; Swanson, M. L. *J. Am. Chem. Soc.* **1984**, *106*, 1883-1884.

(27) Acheson, S. A.; Dedopoulou, D.; Quinn, D. M. *J. Am. Chem. Soc.* **1987**, *109*, 239-245.

Convergent Functional Groups. 8. Flexible Model Receptors for Adenine Derivatives

Tjama Tjivikua, Ghislain Deslongchamps, and Julius Rebek, Jr.*

Contribution from the Departments of Chemistry, University of Pittsburgh, Pittsburgh, Pennsylvania 15260, and The Massachusetts Institute of Technology, Cambridge, Massachusetts 02139. *Received March 30, 1990*

Abstract: The energetics of complexation of highly flexible model receptors with adenine derivatives is reported. These cleftlike receptors, which are complementary to both hydrogen bonding edges of adenine, consist of two imides acylated to an alkyl chain. NMR titration studies reveal that intramolecular hydrogen bonding of these receptors can compete with the chelation of 9-ethyladenine (in $CDCl_3$), resulting in lowered association constants. This phenomenon is probed by comparing the behavior of receptors with alkyl chains of varying lengths. The binding behavior of a triimide derived from tris(2-aminoethyl)amine (tren) is also described.

Introduction

In previous disclosures,[1,2] we have described the synthesis and binding behavior of model receptors for adenine. The synthetic receptors featured aromatic surfaces for π-stacking interactions and imide functions that provided the base pairing. The hydrogen bonding and aryl stacking components provided by these relatively rigid systems could be evaluated simultaneously. Here, we describe the new behavior that arises from the use of flexible spacer groups in structures for adenine recognition.

In searching for an ideal *chelate* for adenine, we had found that structures **1a,b** derived from a 2,7-disubstituted naphthalene spacer provided simultaneous Watson-Crick, Hoogsteen, and aromatic stacking possibilities (Scheme I). Their affinity for adenine

* To whom correspondence should be addressed at the Massachusetts Institute of Technology.

(1) Askew, B.; Ballester, P.; Buhr, C.; Jeong, K.-S.; Jones, S.; Parris, K.; Williams, K.; Rebek, J., Jr. *J. Am. Chem. Soc.* **1989**, *111*, 1082-1090. Rebek, J., Jr.; Askew, B.; Buhr, C.; Jones, S.; Nemeth, D.; Williams, K.; Ballester, P. *J. Am. Chem. Soc.* **1987**, *109*, 5033-5035. Rebek, J., Jr.; Askew, B.; Ballester, P.; Buhr, C.; Costero, A.; Jones, S.; Williams, K. *J. Am. Chem. Soc.* **1987**, *109*, 6866, 6867. Rebek, J., Jr.; Williams, K.; Parris, K.; Ballester, P.; Jeong, K.-S. *Angew. Chem., Int. Ed. Engl.* **1987**, *26*, 1244, 1245.

(2) Benzing, T.; Tjivikua, T.; Wolfe, J.; Rebeck, J., Jr. *Science* **1988**, *242*, 266, 267.

0002-7863/90/1512-8408$02.50/0